Marcus C. Walden

# High-Frequency Near Vertical Incidence Skywave Propagation

*Findings associated with the 5 MHz Experiment.*

This article collates the findings from the 5 MHz Experiment, a U.K.-based amateur radio project involving a network of beacon transmitters and monitoring stations operating at 5.290 MHz. An analysis of the calibrated received signal-power measurements, together with ionosonde frequency measurements and high-frequency (HF) signal and frequency predictions, led to a number of important results relevant to near vertical incidence skywave (NVIS) communications. The emphasis of this article is on practical aspects of this technique for both professional and amateur users of the HF spectrum.

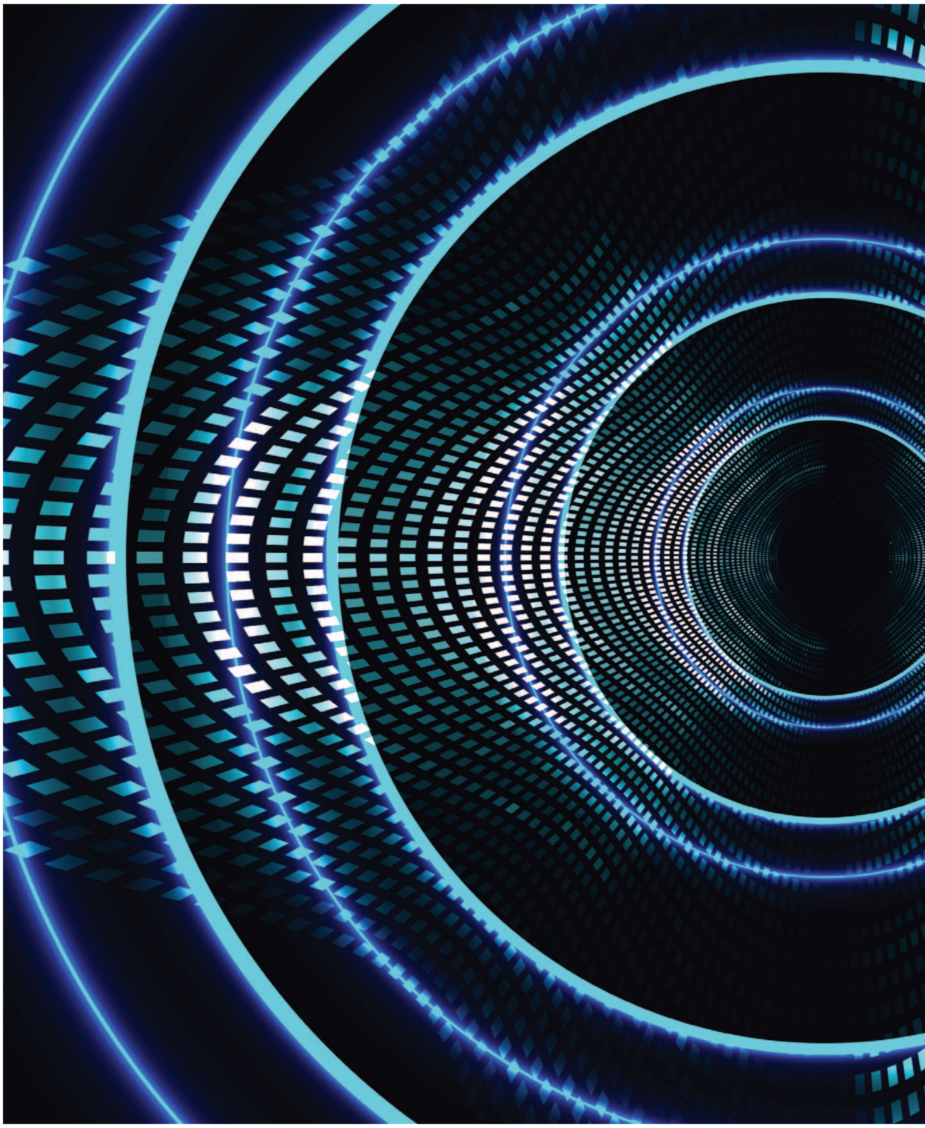

## INTRODUCTION

NVIS propagation allows HF ionospheric communication over relatively short distances, typically up to 400–500 km, using frequencies generally in the range of 2–10 MHz. This technique is important for military and humanitarian organizations as well as amateur radio operators, particularly during emergency situations when the normal power and communications infrastructure may have failed [1]. There can, at times, be substantial overlap between these seemingly disparate NVIS user groups. For example, the Military Auxiliary Radio System in the United

*Digital Object Identifier 10.1109/MAP.2016.2609798*
*Date of publication: 20 October 2016*

 1045-9243/16©2016IEEE 

States consists primarily of civilian radio amateurs supporting military communications [2]. Additionally, the Amateur Radio Emergency Service in the United States and the Radio Amateurs' Emergency Network in the United Kingdom provide volunteer communications for disaster situations as well as community radio services during normal times [3], [4].

This ionospheric-propagation technique primarily makes use of waves transmitted at high angles from the ground such that terrain obstructions (e.g., mountains) have little or no influence on signal strengths. Furthermore, direction finding on waves arriving from high angles is more difficult because bearing errors increase dramatically with decreasing range to the transmitter [5]. Bearing errors arise as a consequence of horizontal gradients in electron density or tilts in the ionosphere [6]. These characteristics make NVIS propagation an important tactical-communications technique at HF, although real-time ray tracing through a tilted ionosphere can lead to more reliable determination of transmitter locations on short-range links [7].

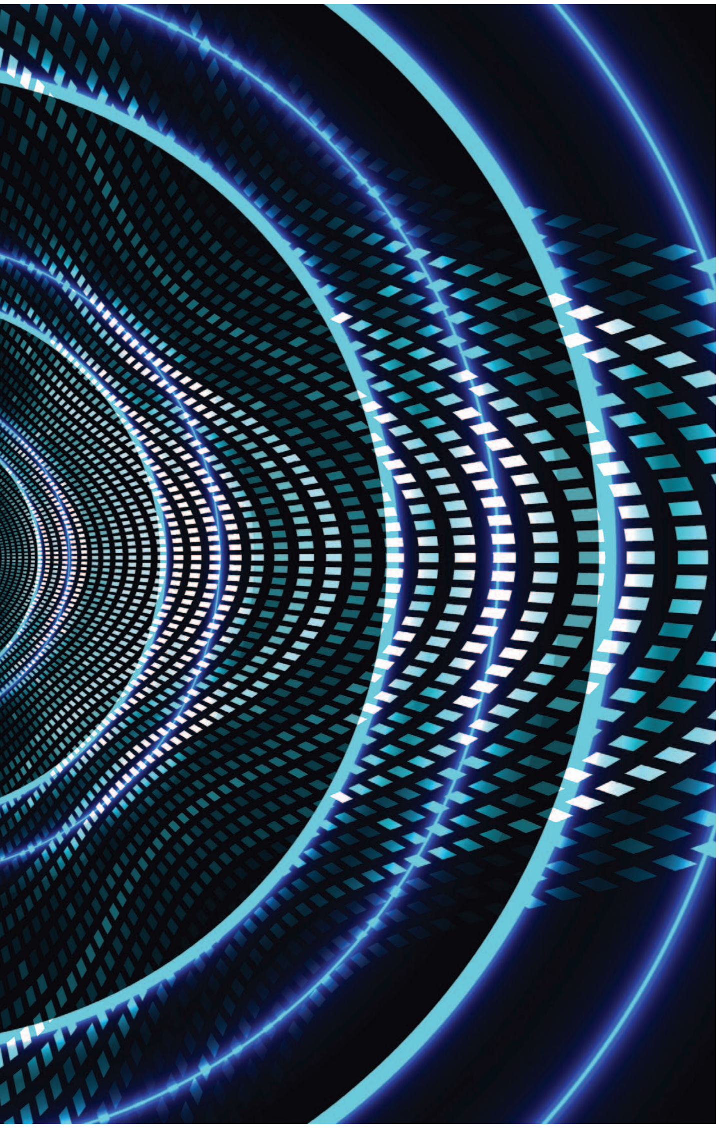



NVIS propagation is predominantly single hop via the F2 region of the ionosphere; therefore, an appropriate choice of operating frequency is important for effective NVIS communications. Additionally, the antenna system needs to be designed to maximize radiation at high elevation angles [1].

The focus of this article is on frequency and signal-level predictions and measurements for NVIS links. Although the regional emphasis is on the United Kingdom, the findings are, in general, relevant to midlatitude locations, which are defined as ~30–60° geomagnetic latitudes, north or south. Discussions on NVIS propagation expand this coverage to a global context.

The details of the 5 MHz Experiment and the associated beacon network that operates at 5 MHz in the United Kingdom are presented. This is an important frequency for midlatitude NVIS communications during daylight hours, particularly at low points in the sunspot cycle when there is insufficient ionization to support propagation at higher frequencies and lower frequencies incur substantial D-region absorption. The importance of 5 MHz for NVIS communications was emphasized by the substantial spectrum negotiations, culminating in a modest secondary allocation at 5 MHz to the amateur service, during the recent World Radiocommunication Conference [8]. Although an amateur radio project, the analysis of calibrated measurements obtained through this experiment resulted in a number of important findings related to NVIS propagation that are of practical relevance to the HF user community, both professional and amateur.

## THE 5 MHz EXPERIMENT

### *OVERVIEW*

In 2002, the U.K. Ministry of Defence and the U.K. communications regulator (Ofcom) allowed radio amateurs access to five 3-kHz-wide channels at 5 MHz under a notice of variation to their licenses. Over the subsequent years, further channels have been made available. The Radio Society of Great Britain, which is the national society promoting the hobby, launched the 5 MHz Experiment to encourage antenna and propagation experimentation at this frequency.

### *TRANSMITTING AND RECEIVING STATIONS*

As part of this project, a network of beacon transmitters was established [9], [10]. A number of radio amateurs established receiving stations for long-term monitoring of the beacon transmitters. I analyzed data from five stations [60].

The call sign, location, and geographic coordinates of the transmitting and receiving stations are listed in Table 1, and Table 2 presents the geographic great-circle range and bearing from each transmitter to each receiving station. In total, there were nine NVIS links (i.e., ground range of <500 km).

Direct-conversion [or zero intermediate-frequency (IF)] receivers were used with the audio output sampled by a computer sound card. Each receiver was calibrated for signal power by its owner. Transmitting antennas are inverted-vee dipoles. Receiving antennas also included inverted-vee dipoles as well as a nonresonant, asymmetric dipole and two electrically small active loops (one tuned and the other broadband). These

**TABLE 1. THE CALL SIGN, LOCATION, AND GEOGRAPHIC COORDINATES OF THE BEACON TRANSMITTING AND RECEIVING STATIONS.**

| Station Type | Call Sign | Location | Geographic Coordinates |
|---|---|---|---|
| Transmitting | GB3RAL | Oxfordshire, United Kingdom | 51.56° N, 1.29° W |
| | GB3WES | Cumbria, United Kingdom | 54.56° N, 2.63° W |
| | GB3ORK | Orkney Isles, United Kingdom | 59.02° N, 3.16° W |
| Receiving | G3SET | Lincolnshire, United Kingdom | 53.39° N, 0.57° W |
| | G3WKL | Buckinghamshire, United Kingdom | 52.10° N, 0.71° W |
| | G4ZFQ | Isle of Wight, United Kingdom | 50.73° N, 1.29° W |
| | G8IMR | Hampshire, United Kingdom | 50.91° N, 1.29° W |
| | GM4SLV | Shetland Isles, United Kingdom | 60.29° N, 1.43° W |

**TABLE 2. THE GEOGRAPHIC GREAT-CIRCLE RANGE (BEARING) FROM THE BEACON TRANSMITTERS TO THE RECEIVING STATIONS [60].**

| Station | G3SET | G3WKL | G4ZFQ | G8IMR | GM4SLV |
|---|---|---|---|---|---|
| GB3RAL | 210 km (14°) | 70 km (33°) | 92 km (181°) | 74 km (180°) | 968 km (0°) |
| GB3WES | 189 km (133°) | 302 km (154°) | 435 km (168°) | 418 km (167°) | 639 km (6°) |
| GB3ORK | 646 km (164°) | 785 km (167°) | 929 km (172°) | 911 km (171°) | 170 km (34°) |

antennas were modeled using Numerical Electromagnetics Code-2 antenna simulation software with appropriate ground electrical characteristics as input [11]. Simulated dipole gains were consistent with previously published measurements of field-deployed antennas [12]. Similarly, simulated loop-antenna gains agreed well with expectations for electrically small loops (e.g., [13]). The effective isotropic radiated power was ~8–23 W depending on the simulated transmitting-antenna gain and the assumed conducted power level [60].

## MAXIMUM FREQUENCY SUPPORTED BY THE IONOSPHERE FOR NVIS PROPAGATION

### *TRADITIONAL NVIS MAXIMUM FREQUENCY DOCTRINE*

Literature describing the practical use of NVIS-propagation techniques emphasizes that the maximum frequency supported by the ionosphere at vertical incidence is *foF*2 (e.g., [1], [5], and [15]). Frequently, *foF*2 is defined as the critical frequency of the ionosphere—as if there were only a single critical frequency—and that the optimum working frequency (OWF) is approximately 0.85 times *foF*2. This doctrine encourages operation at low frequencies, which can lead to spectrum congestion, particularly during sunspot minima when maximum operating frequencies are low in the first place.

This section shows that these traditional NVIS-frequency guidelines are incorrect and oversimplified by considering established ionospheric physics and the underlying theory associated with HF-propagation prediction software. Additionally, signal-to-noise ratio (SNR) measurements from the 5-MHz beacon network are used in support of the already established theory [16]. Finally, I present a reason behind the incorrect use of *foF*2 as the maximum NVIS frequency.

### *THE IONOSPHERE, MAGNETOIONIC THEORY, AND CRITICAL FREQUENCIES*

The ionosphere is a weakly ionized plasma formed in the earth's atmosphere through ionizing radiation—extreme ultraviolet and X-ray radiation—emitted by the sun. The chemical and physical processes associated with the ionosphere, and magnetoionic theory in general, are described in [17]–[19].

Two equations describe radio-wave propagation through the ionosphere: the Appleton equation and the magnetoionic polarization equation [17]. To paraphrase Hunsucker and Hargreaves [20], "it is virtually impossible for an ordinary mortal to make much sense" of these equations "in their full glory." Indeed, it could be argued that the HF user does not need to. However, some knowledge of the salient points could aid in the understanding of NVIS propagation at HF. Of most relevance to this discussion, the equations indicate that two characteristic waves propagate through the ionosphere: the ordinary wave (*O*-wave) and the extraordinary wave (*X*-wave).

These two waves follow different paths through the ionosphere, have orthogonal polarization, and experience different absorption. Additionally, the maximum frequency supported by the ionosphere—termed the *critical frequency*—differs for each characteristic wave, and each region within the ionosphere has critical frequencies associated with it. For example, the F2 region critical frequencies are *foF2* and *fxF2* for the *O*- and *X*-waves, respectively.

The value of *foF2* is directly related to the peak electron density of the F2 region, whereas *fxF2* is also influenced by the earth's magnetic field. The *O*- and *X*-wave critical frequencies for the F2 region are related through [17]

$$foF2^2 = fxF2^2 - fxF2\, f_H, \tag{1}$$

where $f_H$ is the electron gyrofrequency, which depends on the earth's magnetic field strength, also varying with location. If both *foF2* and *fxF2* are much larger than $f_H$, then (1) reduces to the following approximation [17]:

$$fxF2 - foF2 \approx \frac{f_H}{2}. \tag{2}$$

### IONOSONDES AND IONOGRAMS

An ionosonde measures the virtual reflection height of the ionosphere versus frequency. Figure 1 shows an ionogram taken at Chilton, United Kingdom (51.6° N, 1.3° W), using a Digisonde DPS-1 (Lowell Digisonde International, Lowell, Massachusetts) [21]. The red line represents the *O*-wave response, whereas the green line is that for the *X*-wave. The vertical asymptotes relate to their respective critical frequencies.

A model of the bottom-side ionosphere can be obtained through the analysis of the ionogram, usually obtained automatically. Digisonde uses automatic real-time ionogram scaler with true height (ARTIST) software with key parameters tabulated on the left of the ionogram [22]. It has been assumed that ARTIST interpretation errors occur infrequently, although it is noted an expert system for validating ionograms failed about one-third of the time [53]. ARTIST outputs *foF2* but not *fxF2*. A related parameter is *fxI*, which is the maximum recorded F region frequency and provides a measure of the degree of spread F associated with the overhead ionosphere [23]. Spread F is typically a low- or high-latitude phenomenon that gives rise to range or frequency

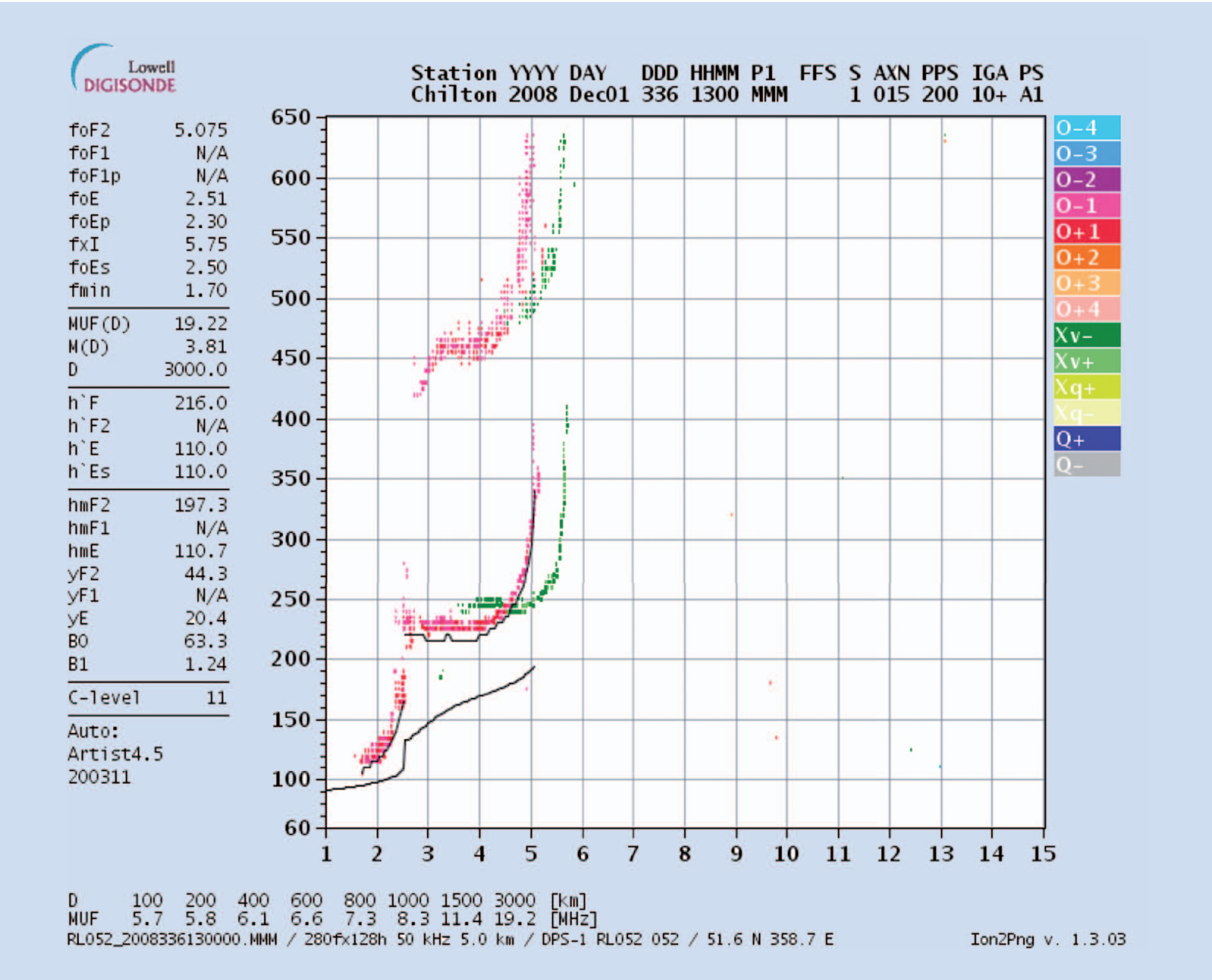


**FIGURE 1.** A Chilton ionogram at 1300 coordinated universal time (UTC) on 1 December 2008 [16].

spread on an ionogram [17]. When spread F is uncommon, the median $fxI$ is equal to the median $fxF2$ [24]. On this assumption, $fxI$ has been used in lieu of $fxF2$ for ionosonde data analysis in this article.

### AMBIGUITY REGARDING THE MAXIMUM USABLE FREQUENCY

At first glance, it would appear that the term *maximum usable frequency* (*MUF*) is easily understood. However, its meaning is very much context dependent with regard to HF ionospheric propagation, which can lead to misinterpretation and misunderstanding. In one case, the MUF is the instantaneous value observed or measured for a given link at a given time and date. In the other, it refers to the monthly median value that is observed or measured. An alternative term for the instantaneous MUF, which I prefer, is the maximum observed frequency (MOF) [25].

The ionogram in Figure 1 also shows predicted MUF values for different length links (distances in kilometers) with Chilton as the midpoint of the link. These are instantaneous MUF, or MOF, values based on a single ionosonde measurement at a given time and date. Of relevance to this discussion is the predicted MUF (5.7 MHz) for a 100-km link (i.e., an NVIS link), which is comparable to the measured $fxI$ (5.75 MHz). In other words, the ionosonde-measured $fxI$, a proxy for the $X$-wave critical frequency, is an indication of the instantaneous MUF/MOF for an NVIS link. By contrast, HF-propagation prediction routines attempt to predict the monthly median MOF, among other parameters.

### PREDICTIONS OF THE MUF

During World War II, the use of HF for short- and medium-range operational purposes intensified, leading to the development of HF prediction methods within a number of organizations, including the Service de Prévision Ionosphérique Militaire in France, the Central Radio Propagation Laboratory of the National Bureau of Standards in the United States, and the Interservices Ionospheric Bureau in the United Kingdom. These methods considered the $X$-wave contribution to the MUF [26], [27].

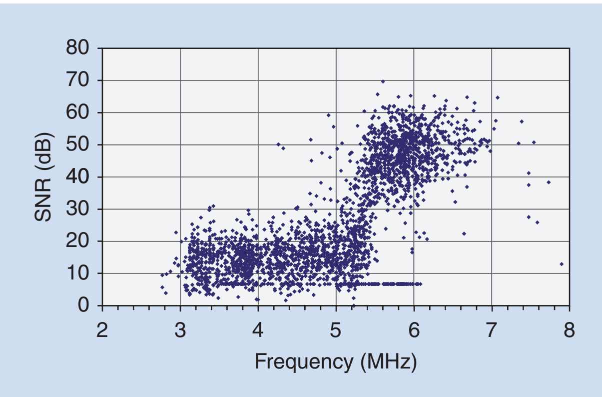


**FIGURE 2.** A measured GB3RAL SNR at G3WKL against Chilton $fxI\sec(\varphi)$ in September 2007 [16].

Over time, HF prediction methods became automated, which enabled the selection of optimum operating frequencies without the use of complicated charts and nomograms. Unfortunately, the automation of these prediction methods has hidden the role of the $X$-wave in MUF predictions from the HF user. Examples of modern HF prediction software include the Advanced Stand Alone Prediction System (ASAPS) [28], the Voice of America Coverage Analysis Program (VOACAP) [25], [29], and the software program associated with International Telecommunication Union Radiocommunication Sector (ITU-R) Recommendation P.533 (ITURHFPROP) [30], all of which can calculate the expected MUF—in this case, the monthly median MOF—for a given link at a given time.

For zero ground distance (i.e., vertical incidence), ASAPS, ITURHFPROP, and VOACAP revert to the same equation to calculate the F2 region MUF,

$$\mathrm{MUF} = foF2 + \frac{f_H}{2}, \tag{3}$$

which is, in effect, the approximation for the $X$-wave critical frequency in (2). The draft *IONCAP Theory Manual* [31] and ITU-R Recommendation P.533 [30] provide more detailed equations for calculating the F2 region MUF for nonzero ground distances that are used in VOACAP and ITURHFPROP (and, effectively, ASAPS).

### SNR MEASUREMENTS USING THE 5-MHz BEACON NETWORK

Comparisons of signal strength and/or SNR measurements from the 5-MHz beacon network with ionosonde measurements clearly show agreement with (3) and that the $O$-wave critical frequency $foF2$ is not the maximum frequency supported by the ionosphere for NVIS links [16]. The latter fact is evident in Figure 2, which shows the peak signal-to-average-noise ratio for GB3RAL measured at G3WKL against the Chilton $fxI\sec(\varphi)$ in September 2007. In this case, $fxI$ has been modified by the secant law because the ionosphere supports higher frequencies for waves at oblique incidence [17]. Although application of the secant law to the ionosonde $foF2$ and $fxI$ measurements is technically correct, it is not entirely necessary for short NVIS links because $\sec(\varphi) \approx 1$ for short ground ranges and reflection from the F2 region.

A near-step increase in SNR occurs only when $fxI\sec(\varphi)$ exceeds the beacon operating frequency of 5.290 MHz, which is consistent with (3) and emphasizes the importance of the $X$-wave in NVIS propagation. By contrast, plotting the same beacon data against $foF2\sec(\varphi)$ (not shown here) would show a near-step increase in SNR at ~4.60 MHz, which contradicts traditional NVIS-frequency guidelines.

### HAPPY HOUR

Recently, Dutch researchers have coined the term *Happy Hour* as the period of time when the ionospheric-propagation path is open with only the $X$-wave propagating [32]. The Happy Hour duration depends on the rate of change of electron density within the ionosphere, which is determined by the season and state of the sunspot cycle. For example, the Happy Hour might be only ~30 min during the winter, whereas it could be a few hours during the summer.

Figure 3 compares the Chilton *foF2* and *fxI* with the sound-card signal level for the GB3RAL beacon received at G4ZFQ in February 2010. The data points represent instantaneous measurements, and the solid lines represent the monthly median of the respective measurements. At ~0730 UTC, the monthly median signal level rises sharply as the monthly median *fxI* exceeds the beacon operating frequency, whereas it is another 30 min before the monthly median *foF2* exceeds the beacon frequency at ~0800 UTC.

During sunspot minima, when electron densities and, therefore, maximum frequencies supported by the ionosphere are low, it is possible that only the *X*-wave is supported at the operating frequency. For example, Figure 4 compares the Chilton *foF2* and *fxI* with the sound-card signal level for the GB3RAL beacon received at G3WKL in January 2009, and, for the majority of this month, the ionosphere supported only the *X*-wave at 5.290 MHz. In this example, the median duration of the Happy Hour is approximately 5.5 h. Again, these data illustrate the relevance of the *X*-wave for NVIS propagation.

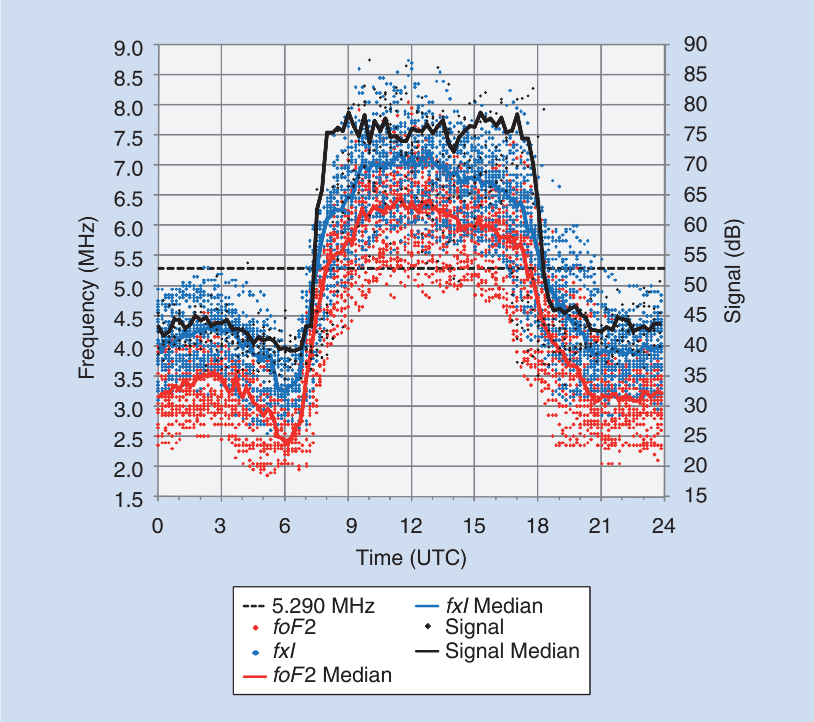


**FIGURE 3.** A comparison of Chilton *foF2* and *fxI* and the measured sound-card signal level for GB3RAL received at G4ZFQ in February 2010.

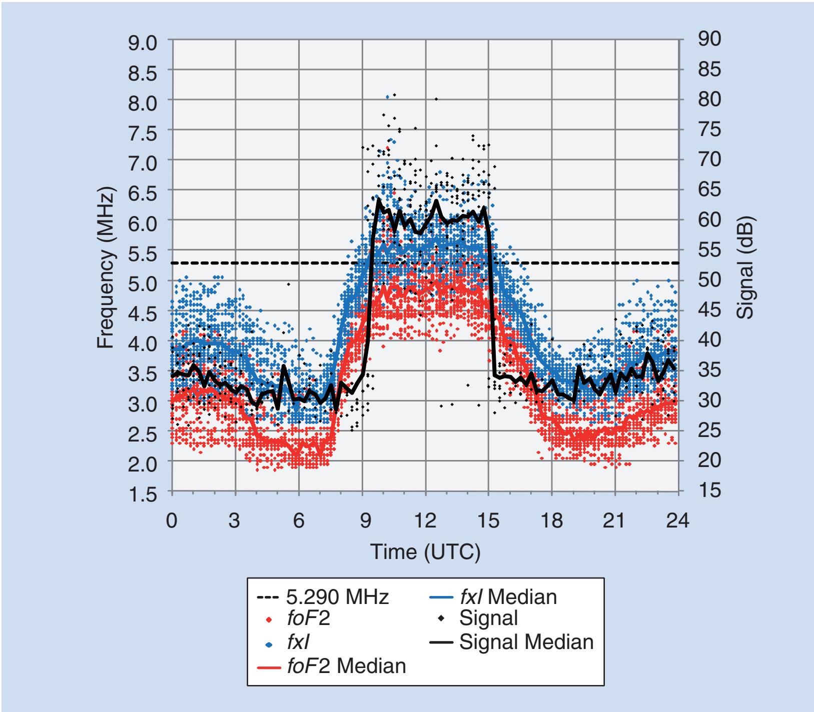


**FIGURE 4.** A comparison of Chilton *foF2* and *fxI* and the measured sound-card signal level for GB3RAL received at G3WKL in January 2009.

## COMPLICATIONS ASSOCIATED WITH THE IONOSPHERE

### IONOSPHERIC VARIABILITY

Median curves derived from measurements over a long period of time (e.g., one month) typically show smooth characteristics that mask any short-term variability. Median measurements show good long-term correlation with the smoothed sunspot number (SSN)—a useful and convenient solar index derived from monthly observed sunspot numbers averaged over a 12-month period—but the short-term correlation is poor because solar flux characteristics exhibit chaotic behavior [33]. The National Oceanic and Atmospheric Administration provides seven-day plots of *foF2*, in which general trends are obvious [34]. Typical Chilton measurements would show *foF2* as greatest around midday and lowest in the night during winter months, but there would also be an indication of the critical frequency variability that can arise over relatively short time periods (e.g., frequency changes of a few hundred kilohertz in <1 h).

## ABSORPTION

Collisions among electrons, neutral molecules, and ionized particles within the ionosphere result in absorption of radio-wave energy. Ionospheric absorption can be defined as nondeviative and deviative. For nondeviative absorption, the *X*-wave experiences greater absorption than the *O*-wave, particularly at frequencies approaching the electron gyrofrequency [17]. This effect can be observed on daytime ionograms, where *X*-wave returns lower than ~4 MHz are not present owing to substantial D-region absorption (for example, see Figure 1). Deviative absorption occurs when the operating frequency at vertical incidence is close to the critical frequency, and its effect is shown in Figure 2 as a ramp-up in SNR rather than a step change once $fxI\sec(\varphi)$ exceeds the beacon transmit frequency. At lower frequencies, excessive absorption renders the *X*-wave ineffective, whereas absorption of the two waves is comparable above ~5–8 MHz [35].

**The guideline that *foF2* is the maximum vertical-incidence frequency is location specific.**

## POLARIZATION

Wave polarization depends on geomagnetic latitudes and angles of incidence. A wave entering the ionosphere separates into the two characteristic waves. The region at the bottom of the ionosphere is the limiting region because the polarization of a downcoming wave no longer varies with height once it passes below, and the polarization acquired here is the limiting polarization [36]. Polarization is circular at a magnetic dip pole (i.e., ±90°), whereas the two characteristic waves are linearly polarized at the magnetic dip equator. In the latter case, an antenna aligned north–south excites only an *O*-wave, whereas it excites only the *X*-wave when aligned east–west [17]. At midlatitude locations, these waves are elliptically polarized with opposite senses of rotation; polarization becomes highly elliptical at medium frequencies, whereas it tends to circular polarization at higher frequencies [37].

The sense of rotation for circular polarization is described as either left- or right-hand circular polarization. Unfortunately, two definitions for the sense of rotation exist: a classical optics definition and the IEEE definition [38]. Budden [39] emphasized that care is required when interpreting work by other authors on wave polarization through the ionosphere.

Some classic ionospheric texts (e.g., [17] and [18]) describe the sense of rotation relative to the direction of the magnetic field, presumably to avoid any confusion about the polarization. Davies [17] provides a useful rule for remembering the sense of rotation: "When the thumb points in the direction of the magnetic field $B_0$, the rotation of the extraordinary-wave vectors is given by the fingers of the right hand; the rotation of the ordinary-wave vectors is given by the fingers of the left hand." It is evident that the polarization of the upward wave is opposite that of the downward wave at vertical incidence. Although not commonly described in HF literature, Witvliet [40] refers to this fact.

For a linearly polarized upward wave at vertical incidence at midlatitudes, the power is divided approximately evenly between each characteristic wave. At frequencies where absorption is similar for the *O*- and *X*-waves, received power levels will be comparable, which can result in polarization fading if these two waves recombine in the limiting region to form a linearly polarized wave. The resultant electric field rotates over time in a manner related to the total electron content of the path through the ionosphere. This effect is known as a *Faraday rotation* [17].

## RADIO NOISE

External noise sources—atmospheric, galactic, and man-made—tend to limit HF-receiver sensitivity. Owing to the simultaneous presence of multiple strong signals, HF receivers do not, as a rule, have low noise figures but instead require good strong-signal-handling capabilities [41].

Generally, noise levels decrease as the operating frequency increases [42]. The existing frequency-of-optimum-traffic (FOT) guideline encourages operation at lower frequencies where noise levels might be higher. Operation at higher frequencies might yield an improved SNR, although the path loss is less at lower frequencies, which would offset the increased noise to some extent.

## *CONUNDRUM REGARDING EMPHASIS ON foF2*

These results raise the question as to why traditional NVIS literature has placed the emphasis on the *O*-wave critical frequency *foF2* as being the highest frequency supported by the ionosphere. An explanation is offered that, to the best of my knowledge, has not previously been presented.

Substantial work relating to NVIS propagation—specifically, quasi-transverse propagation—was carried out by U.S. researchers during the Vietnam War in the 1960s and 1970s (e.g., [43]–[45]). This part of Southeast Asia is very close to the magnetic dip equator, where the limiting polarization of the characteristic waves at vertical incidence is linear and where there would be a risk of polarization mismatch if linearly polarized NVIS antennas were oriented orthogonal to each other. Nacaskul [45] showed that excitation of the *O*-wave (i.e., north–south alignment) generally produced stronger signals than when the *X*-wave was excited (i.e., east–west alignment), which led to the primary recommendation that antennas should be aligned north–south. In the event that the *O*-wave is not supported on a particular frequency, then east–west alignment should be tried if diversity systems are available.

I believe that it is highly unlikely—not to mention impractical—that soldiers under difficult wartime conditions would experiment with antenna orientation. The simplest and lowest-risk approach would be to orientate antennas north–south for *O*-wave excitation alone. Consequently, the *O*-wave critical frequency *foF2* would be the maximum frequency supported by the ionosphere under this antenna configuration. The guideline that *foF*2 is the maximum vertical-incidence frequency is location specific. However, over time, this guideline has been applied in a global context, and its technical origins appear to have been forgotten.

**To identify the MOF (or at least refine the MOF estimate), some form of real-time channel evaluation is required.**

### *MAXIMUM NVIS-OPERATING-FREQUENCY GUIDELINES*

A MOF-seeking approach should be adopted when selecting NVIS operating frequencies to maximize the received SNR with the additional benefit of reducing congestion at lower frequencies [5]. To identify the MOF (or at least refine the MOF estimate), some form of real-time channel evaluation is required. Ionosondes could be used for NVIS links, but automatic link establishment (ALE) systems, in which a bank of channels is sounded to identify the channel with the best link quality, have become the norm [46]. ALE systems have evolved over recent years to a third generation capable of supporting wide-band-HF-modulation schemes [47]. Lane [48] provided guidelines for selecting the range of suitable ALE frequencies based on HF-propagation prediction tools.

Owing to ionospheric variability as well as increased deviative absorption, it would be prudent not to operate too closely to the NVIS MOF in case of a rapid loss of signal. Additionally, wave polarization (which is frequency and location dependent) and antenna orientation need to be considered. Ultimately, the amount of frequency margin required will depend on consideration of these different parameters, how critical a given link is, and for how long a link outage could be tolerated before the link is reestablished.

## COMPARISON OF IONOSONDE VERTICAL-INCIDENCE MEASUREMENTS WITH HF-PROPAGATION PREDICTIONS

### *BACKGROUND*

In the design of an NVIS system, the selection of a good operating frequency is important. If the operating frequency is too high, then the radio waves simply penetrate the ionosphere, whereas if it is too low, absorption might be excessive. HF-prediction software facilitates the choice of frequencies. This section compares Chilton ionosonde frequency measurements with ASAPS and VOACAP frequency predictions [49], [54].

### *FREQUENCY DEFINITIONS RELATING TO MONTHLY MEDIAN VALUES*

HF-propagation prediction software such as ASAPS and VOACAP attempt to predict the statistical spread of usable frequencies for a given link over a set time period (usually one month). ITU-R Recommendation P.373 provides definitions of maximum and minimum transmission frequencies relevant to HF-propagation predictions, including the MUF, which is a median value (i.e., monthly median MOF) [5], [50].

The OWF and the highest probable frequency (HPF) exceed the MUF in 90% and 10% of the specified period, respectively. In this context and assuming that one month has 30 days, the OWF is expected to be supported on 27 days of a month, whereas the HPF should be available on three days of the month. Consequently and potentially confusing, it is possible for operation at frequencies above the MUF (ATM).

The OWF is a misleading term because there is no indication as to the performance or quality of service [51]. In other words, system performance may not be optimum at the OWF. The merit of the OWF is perhaps best understood when considering frequency allocations from a licensing perspective. If only one frequency were to be made available and there was an expectation that the frequency must be supported on most days of the month (e.g., 90% of days), then the OWF would be the frequency of choice.

### *HF PREDICTIONS AND CHILTON IONOSONDE MEASUREMENTS*

The ASAPS and VOACAP vertical-incidence-frequency predictions were compared with Chilton ionosonde measurements from 1996 to 2010 [49]. VOACAP method 9 predicts the MUF, HPF, and FOT (equivalent to the OWF) and uses the SSN as the solar index to drive predictions [25]. ASAPS predicts the MUF, OWF, and upper decile (UD; equivalent to the HPF) and uses the T index (an effective sunspot number based on global ionosonde *foF*2 measurements) to drive its frequency predictions. [52]. The HF MUF predictions were compared with the monthly median *foF*2 and *fxI* on a month-by-month basis. Likewise, the predicted OWF/FOT and UD/HPF were compared with the measured lower-decile (LD) and UD frequencies respectively.

### *COMPARISON RESULTS*

ASAPS tended to predict the *X*-wave critical frequency, thereby showing consistency with (3), whereas VOACAP was more conservative in its prediction of the MUF (i.e., VOACAP predicted lower frequencies). The average differences between the measured and predicted MUF from 1996 to 2010 inclusive are presented in Table 3.

Both ASAPS and VOACAP (the latter more so) were conservative in their predictions of the LD frequencies. For the UD frequencies, ASAPS again showed consistency with (3), whereas VOACAP was again conservative in its frequency prediction.

ALE-frequency–planning guidelines recommend the use of frequencies from just below the lowest FOT/OWF up to the highest HPF/UD [48]. From this analysis, ASAPS appears to be a better choice than VOACAP for preparing ALE-frequency scan lists for U.K. NVIS links.

Statistics summarized in a single table fail to describe multiple facets observed over a complete solar cycle. For example, both the ASAPS- and VOACAP-predicted MUF tended toward *foF2* lower than ~4 MHz during winter months, particularly around the sunspot minimum. These discrepancies could be due to Chilton autoscaled *foF2* values exhibiting positive errors at low frequencies [54], [55]. Spread F might also contribute to the observed inconsistency with (3). Although spread F is typically a low- and high-latitude phenomenon, high-latitude spread F begins at ~40° geomagnetic latitude. Furthermore, high-latitude spread F occurs mostly during the night [37]. Nighttime vertical-incidence frequencies during the winter tend to be low (i.e., <4 MHz). A recent study presents the statistics of nighttime spread F observed at a midlatitude location over a full solar cycle [56].

From 1996 to 2010, ASAPS MUF predictions were within ~10% of *fxF2*, except at low or negative values of the T index.

**Although the SSN can be useful for long-term forecasting of HF propagation, the sun's chaotic behavior makes short-term forecasting more difficult using daily sunspot numbers.**

**TABLE 3. THE AVERAGE DIFFERENCES BETWEEN THE MEDIAN CHILTON MEASUREMENTS AND PREDICTIONS (1996–2010) [49].**

| Measurement (50%) | Prediction | Mean (MHz) | Standard Deviation (MHz) |
|---|---|---|---|
| *fxI* | ASAPS MUF | 0.09 | 0.25 |
| *foF2* | | –0.65 | 0.25 |
| *fxI* | VOACAP MUF | 0.48 | 0.31 |
| *foF2* | | –0.25 | 0.30 |

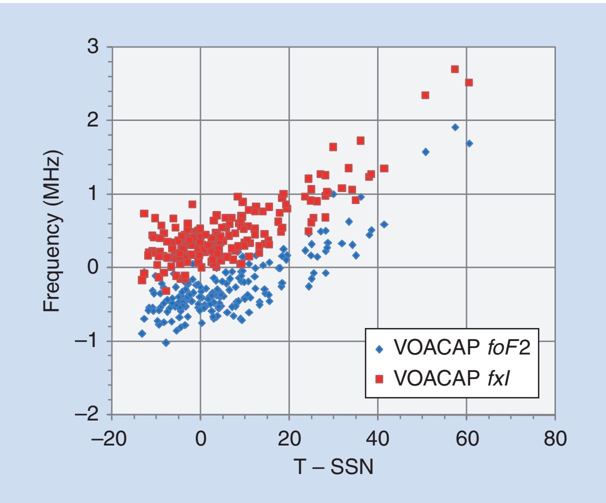


**FIGURE 5.** The monthly mean difference between Chilton measurements and the VOACAP MUF against T – SSN [49].

VOACAP was relatively consistent, albeit conservative, in its prediction of the MUF, except for high SSNs (i.e., more than ~100). VOACAP is likely to be inaccurate or overly pessimistic for MUF predictions on U.K. NVIS links when the difference between the T index and SSN (i.e., T – SSN) exceeds ~15, as illustrated in Figure 5.

Although the SSN can be useful for long-term forecasting of HF propagation, the sun's chaotic behavior makes short-term forecasting more difficult using daily sunspot numbers. Predictions using ersatz indices (e.g., T index) are known to outperform predictions using direct indices such as the SSN. Furthermore, the sunspot number is only a circumstantial index with regard to predicting ionospheric propagation [5]. Goodman [33] suggested that taking a five-day average of effective sunspot numbers strikes a good balance.

## COMPARISON OF 5-MHz BEACON MEASUREMENTS WITH HF-PROPAGATION PREDICTIONS

### OVERVIEW

Some limited work has compared SNR measurements with VOACAP predictions for NVIS links [57]. Another study compared median signal-power measurements, including a 490-km NVIS link, with ASAPS and VOACAP predictions over a ten-month period [58].

Since its inception, a large database of automatic beacon measurements has resulted from the 5 MHz Experiment. The early analysis of beacon data indicated that high-reliability (i.e., >90%) NVIS links could be achieved using narrow-band modes (e.g., below ~500 Hz) at typical man-pack power levels (e.g., 10–20 W) when received in low-noise environments [14]. It was also found that SNR measurements could be strongly affected by cochannel interference, even over one month. For example, SNR measurements for the GB3ORK-GM4SLV link in November 2009 showed a notch in the SNR between ~1200 and 1300 UTC, which was probably caused by regular cochannel interference. For this reason, signal-power levels were analyzed instead of the SNR. This section compares the measured signal-power levels against those predicted by ASAPS and VOACAP for nine NVIS links over a 23-month period from May 2009 to March 2011 during the last sunspot minimum [59], [60].

### PREDICTIONS OF MEDIAN SIGNAL-POWER LEVELS

VOACAP predictions used method 20 (complete system performance) with Consultative Committee on International Radio coefficients and the SSN as input. The VOACAP sporadic E model was not enabled [25]. The ASAPS T index was negative for some months, meaning that the observed ionospheric conditions were worse than expected for the nonzero, positive SSN.

In view of the transmitting- and receiving-antenna types used, the ASAPS approximation algorithm was used to determine median signal levels [28]. The ASAPS and VOACAP hourly predictions were interpolated to 15-min intervals to coincide with the beacon transmit interval.

### COMPARISON OF SIGNAL-LEVEL MEASUREMENTS AND PREDICTIONS

Figure 6 shows an example of signal measurements and the corresponding ASAPS and VOACAP median signal predictions observed for the GB3RAL-G3WKL link in March 2010. Differences tend to increase at the start and end of NVIS propagation, corresponding to a low ASAPS probability or VOACAP MUFday. Signal-level measurements show a small spread during the day. This particular example shows very good correlation between median measurements and predictions. However, some measurements for other months show less agreement. The statistics from all nine NVIS links were viewed together. If taken in isolation, measurements showing large differences from predictions could be viewed as being in error.

The root-mean-square (rms) difference between the median signal levels and predictions when VOACAP MUFday and ASAPS probability were >0.03 (i.e., ionospheric support for the primary mode is expected on at least one day in the month) appeared to show a cyclical trend, which was much more apparent when limiting the comparison to a smaller time window at approximately 1200 UTC, as shown in Figure 7 for VOACAP predictions. The rms differences were low in September, October, November, and March. By contrast, the rms differences were larger during the day in the summer months (April to August) and during the winter (December to February). ASAPS predictions showed greater rms differences than VOACAP during the summer but lower rms differences during the winter.

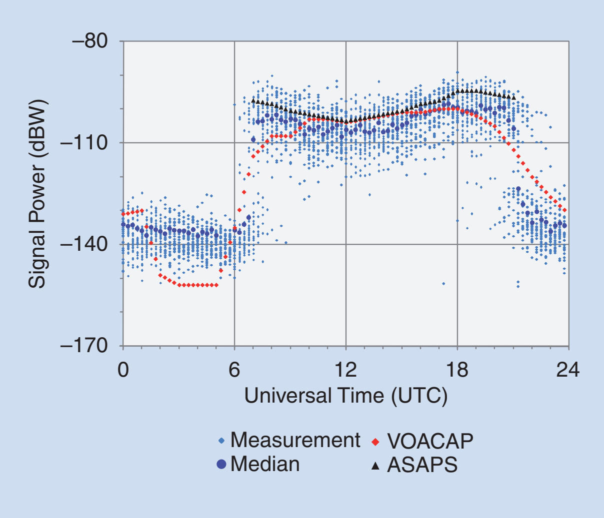


**FIGURE 6.** A comparison of measurements and predictions for GB3RAL received at G3WKL in March 2010 [60].

The summer differences could be related, in part, to the absorption effects (both deviative and nondeviative). The greater spread in signal levels during the summer daytime suggests the presence of multiple propagation modes, including sporadic E, which might have influenced the measurement statistics. The greater absorption observed in December, January, and February is consistent with the winter anomaly when there is anomalously high absorption.

Table 4 presents the range of mean differences and the overall rms differences. Both ASAPS and VOACAP appeared to overestimate the median signal level for the NVIS links at 5.290 MHz, based on the assumption that the prediction-input and antenna-modeling parameters were valid. On the whole, VOACAP showed slightly lower rms and mean differences between the measurements and predictions than ASAPS for

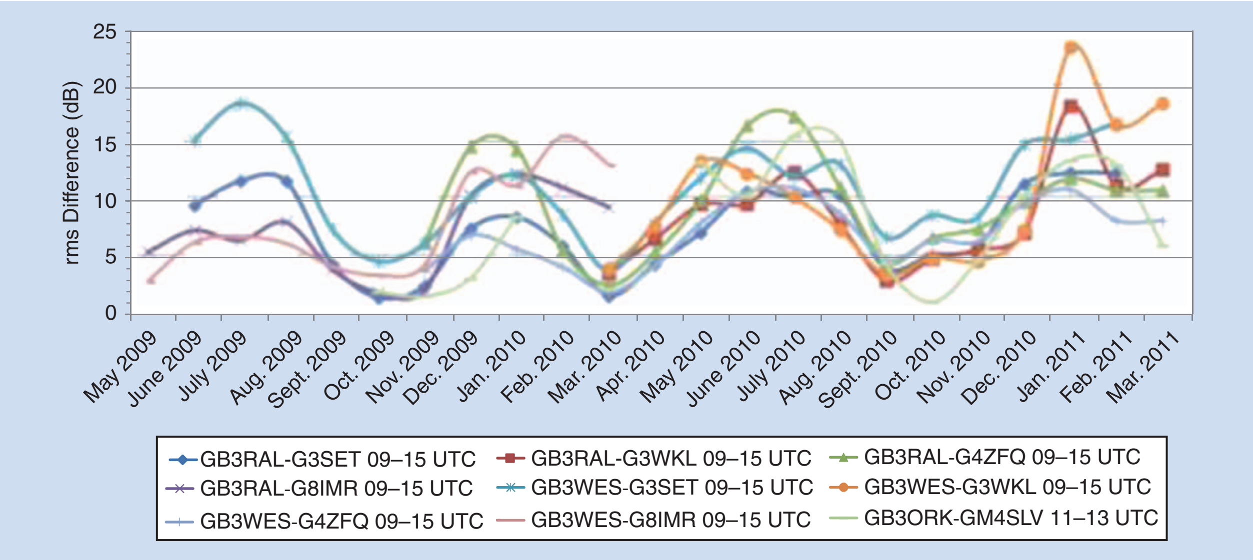


**FIGURE 7.** The rms difference between measurements and VOACAP predictions for a window at approximately 1200 UTC [60].

**TABLE 4. THE RANGE OF MEAN DIFFERENCES BETWEEN THE MEASUREMENTS AND PREDICTIONS FOR ALL LINKS DURING THE MEASUREMENT PERIOD [60].**

| | VOACAP (MUFday > 0.03) | ASAPS (Probability > 0.03) | VOACAP (~1200 UTC) | ASAPS (~1200 UTC) |
|---|---|---|---|---|
| Mean (dB) | −4 to −12 | −8 to −14 | −6 to −11 | −6 to −12 |
| Overall rms (dB) | 7–15 | 9–16 | 7–12 | 7–13 |

these NVIS links at 5.290 MHz over a 23-month period during the recent solar minimum.

## ATM PROPAGATION

### BACKGROUND

The beacon measurements frequently showed evidence of ATM propagation during the night when valid signal measurements were recorded. During this period, ASAPS probability and VOACAP MUFday predictions were zero (i.e., ionospheric support of the primary mode was not predicted). Measured critical frequencies at Chilton were below the operating frequency. The propagation mechanism was not NVIS but might have been a two-hop ground (or sea) side-scatter mode [61]. The median signal levels were generally 30–40 dB lower than the typical daytime levels. Therefore, these links might have been more effective at lower operating frequencies, where true NVIS propagation would actually have been supported by the ionosphere.

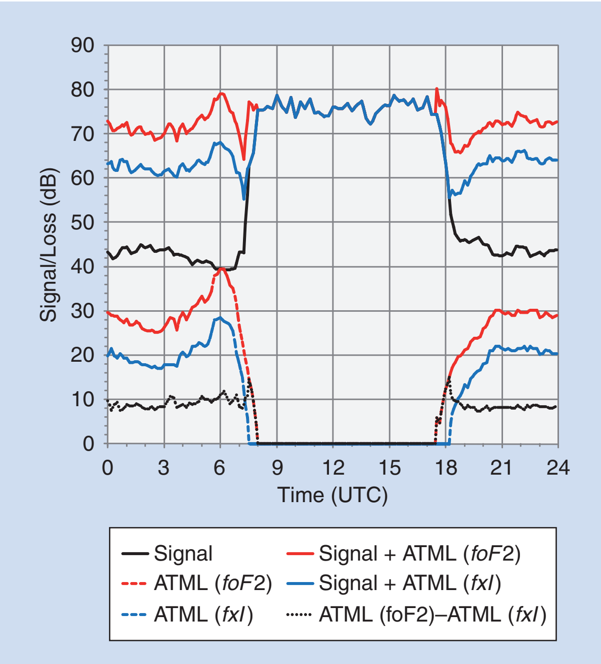


**FIGURE 8.** A comparison of the measured signal (black line), the predicted ATM loss (ATML; dashed red and blue lines), the measured signal adjusted for the predicted ATM loss (solid red and blue lines), and the difference between the predicted ATM losses (dotted black line) using the measured Chilton *foF2* and *fxI* for GB3RAL received at G4ZFQ in February 2010.

### PREDICTION OF ATM LOSS

The ITU-R describes various propagation mechanisms that may give rise to propagation above the basic MUF (ABM) as well as a number of loss models, including the ITU-R Recommendation P.533 model [62]. Until recently, for F2 modes up to a range of 7,000 km, the ABM-loss model was given by [63]

$$L_m = 36\left[\left(\frac{f}{f_b}\right) - 1\right]^{\frac{1}{2}} \tag{4}$$

or 62 dB, whichever is smaller. The working frequency is given by $f$, and $f_b$ is the basic MUF.

The latest version of ITU-R Recommendation P.533 at the time of writing this article predicts 5 dB of additional loss, although no information was provided regarding this change [30]:

$$L_m = 36\left[\left(\frac{f}{f_b}\right) - 1\right]^{\frac{1}{2}} + 5. \tag{5}$$

The purpose of predicting the ATM/ABM losses is less useful for SNR and reliability predictions on wanted links. Instead, the primary interest is for the prediction of interfering signal levels [64].

VOACAP incorporates an ATM-loss model, although the maximum ATM-loss limit is only 25 dB, which may be too low [65]. Related to this ATM-loss limit, it was found that VOACAP reliability predictions can be in error for short-range links at substantially ATM frequencies. Under these circumstances, users should carry out their own validation of the prediction data [66].

### COMPARISON OF MEASURED BEACON-SIGNAL LEVELS AND PREDICTED ATM LOSS USING IONOSONDE FREQUENCY MEASUREMENTS

The ITU-R ABM loss was calculated using (4) with the Chilton median *foF2* and *fxI*—*fxI*, in lieu of *fxF2*—as the basic MUF values. The median beacon-signal level against time was then adjusted by the predicted ABM loss.

Figure 8 shows the median signal level for the GB3RAL beacon received at G4ZFQ (solid black line) as well the predicted ABM loss using the median *foF2* and *fxI* in February 2010. The ABM loss using *foF2* (dashed red line) was evidently greater than that using *fxI* (dashed blue line), which is to be expected considering (1) and (2). Modifying the beacon-signal level by the predicted ABM losses resulted in the solid red and blue lines using the *foF2* and *fxI* measurements, respectively, as the basic MUF in (4).

The solid red line in Figure 8 uses the median *foF2* value to predict the ABM loss. When ATM propagation occurs, the

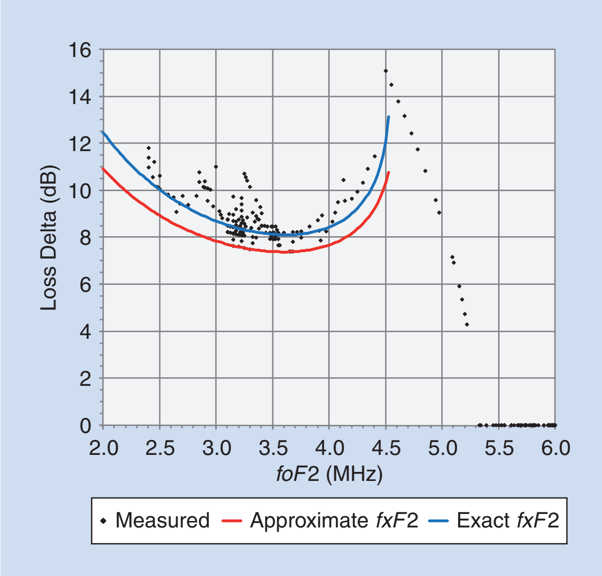


**FIGURE 9.** A comparison of the difference between the ATM losses calculated using Chilton *foF2* and *fxI* and the expected differences when using the approximate and exact expressions for *X*-wave critical frequency *fxF2* against Chilton *foF2* in February 2010.

adjusted beacon-signal level is comparable to the unadjusted signal level during the day (~0800–1700 UTC). Inspection of Figure 8 suggests that use of (5) might provide better agreement than (4). The dotted black line shows the difference between the predicted ABM losses using *foF2* and *fxI*. The latter data are plotted against the Chilton *foF2* in Figure 9. Also shown are the expected differences using the exact (blue line) and approximate (red line) expressions as given by (1) and (2), respectively. There is good agreement when the exact relationship given by (1) is used.

This analysis indicates that there is an inconsistency with the current ITU-R Recommendation P.533 with regard to the basic MUF term. The calculation of the basic MUF tends to the *X*-wave critical frequency *fxF2* for zero ground distance (i.e., NVIS links). However, the ABM-loss model appears to agree well with measurements when the *O*-wave critical frequency *foF2* is used as the basic MUF. Using *fxF2* (or *fxI*) as the basic MUF in (4) or (5) underpredicts the ATM/ABM loss by ~8–14 dB. This difference may be relevant for predictions of interference from nearby transmitters.

## SUMMARY

This article presented numerous findings obtained through the analysis of beacon-signal-power measurements from the 5 MHz Experiment. These important findings relate to

1) maximum NVIS-operating-frequency definitions
2) U.K. NVIS-frequency predictions
3) U.K. NVIS-signal-power predictions
4) ITU-R above-the-loss models.

The findings are of practical relevance to professional and amateur users of NVIS-communications techniques.


## ACKNOWLEDGMENTS

Numerous people have made substantial contributions to the 5 MHz Experiment, without which I would not have been able to carry out any data analysis. Those involved include Peter Martinez (G3PLX), Andrew Talbot (G4JNT/G8IMR), Michael Willis (G0MJW), John Linford (G3WGV), John Grieve (GM0HTH), David Aram (G3SET), John Gould (G3WKL), Alan Reeves (G4ZFQ), and John Pumford-Green (GM4SLV). The Radio Society of Great Britain coordinated the experimentation at 5 MHz and hosted the 5-MHz database. The U.K. Ministry of Defence and Ofcom allowed radio amateurs access to specific channels at 5 MHz.


## AUTHOR INFORMATION


***Marcus C. Walden*** (marcus.walden@plextek.com) received his B.Eng. (Hons) degree in electronic and electrical engineering in 1990 and his Ph.D. degree in microwave engineering in 1994 from the University of Leeds, United Kingdom. From 1995 to 1997, he was a radar engineer with the British Antarctic Survey, developing an airborne, very high-frequency (HF) radar system for measuring ice depth in the Antarctic. He is currently the technical lead of antennas and propagation with Plextek, Great Chesterford, United Kingdom. His research interests include antennas and propagation from HF to millimeter-wave frequencies. He is a Senior Member of the IEEE.


## REFERENCES


[1] D. M. Fiedler and E. J. Farmer, *Near-Vertical Incidence Skywave Communications: Theory, Techniques and Validation*. Sacramento, CA: Worldradio Books, 1996.

[2] United States Army. Military Auxiliary Radio System. [Online]. Available: http://www.usarmymars.org/

[3] American Radio Relay League. Amateur Radio Emergency Service. [Online]. Available: http://www.arrl.org/ares

[4] Radio Amateurs' Emergency Network. [Online]. Available: http://www.raynet-uk.net/

[5] J. M. Goodman, *HF Communications: Science and Technology*. New York: Reinhold, 1992.

[6] L. F. McNamara, *The Ionosphere, Communications, Surveillance, and Direction Finding*. Melbourne, FL: Krieger, 1991.

[7] X. Huang and B. W. Reinisch, "Real-time HF ray tracing through a tilted ionosphere," *Radio Sci.*, vol. 41, no. 5, p. RS003378, Oct. 2006.

[8] International Amateur Radio Union (2015). Amateur radio: The greatest of all scientific hobbies. [Online]. Available: http://www.iaru-r1.org/index.php/3-news/newsflash/1492-new-band-at-5-mhz

[9] A. Talbot, "Design and construction of the 5 MHz beacons GB3RAL, GB3WES and GB3ORK—Part one," *RadCom*, vol. 81, no. 6, pp. 85–87, June 2005.

[10] A. Talbot, "Design and construction of the 5 MHz beacons GB3RAL, GB3WES and GB3ORK—Part two," *RadCom*, vol. 81, no. 7, pp. 88–89, July 2005.

[11] G. J. Burke and A. J. Poggio, "Numerical Electromagnetics Code (NEC)—Method of moments," Lawrence Livermore National Laboratory, Livermore, CA, Rep. UCID-18834, Jan. 1981.

[12] G. H. Hagn, "On the relative response and absolute gain toward the zenith of HF field-expedient antennas—Measured with an ionospheric sounder," *IEEE Trans. Antennas Propag.*, vol. 21, no. 4, pp. 571–574, July 1973.

[13] B. A. Austin, A. Boswell, and M. A. Perks, "Loss mechanisms in the electrically small loop antenna," *IEEE Antennas Propag. Mag.*, vol. 56, no. 4, pp. 142–147, Aug. 2014.

[14] M. C. Walden, "A comparison of measurements and propagation simulations for mid-latitude HF NVIS links at 5 MHz during sunspot minima," in *Proc. 9th Nordic HF Conf. HF 10*, Fårö, Sweden, 2010.

[15] N. Maslin, *HF Communications: A System Approach*. London: Sir Isaac Pitman, 1987.

[16] M. C. Walden, "The extraordinary wave mode: Neglected in current practical literature for HF NVIS communications," in *Proc. Inst. Engineering and Technology 11th Int. Conf. Ionospheric Radio Systems and Techniques*, Edinburgh, U.K., 2009, pp. 27–31.

[17] K. Davies, *Ionospheric Radio*. Stevenage, U.K.: Peregrinus, 1990.

[18] J. K. Hargreaves, *The Solar-Terrestrial Environment*. Cambridge, U.K.: Cambridge Univ. Press, 1995.

[19] J. A. Ratcliffe, *The Magneto-Ionic Theory and Its Applications to the Ionosphere*. Cambridge, U.K.: Cambridge Univ. Press, 1959.

[20] R. D. Hunsucker and J. K. Hargreaves, *The High-Latitude Ionosphere and Its Effects on Radio Propagation*. Cambridge, U.K.: Cambridge Univ. Press, 2002.

[21] Lowell Digisonde International. [Online]. Available: http://www.digisonde.com/index.html

[22] I. A. Galkin and B. W. Reinisch. (2008, Jan. 23). The new ARTIST 5 for all digisondes. *INAG Bull.* [Online]. *(24)*. Available: http://www.sws.bom.gov.au/IPSHosted/INAG/web-69/2008/artist5-inag.pdf

[23] Ionospheric Network Advisory Group. (1969, Sept.) Ionosphere station information bulletin. *INAG Bull.* [Online]. Available: http://www.sws.bom.gov.au/IPSHosted/INAG/pdf/inag01.pdf

[24] Ionospheric Network Advisory Group. (1971, Aug.) Ionosphere station information bulletin. *INAG Bull.* [Online]. Available: http://www.sws.bom.gov.au/IPSHosted/INAG/pdf/inag08.pdf

[25] G. Lane, *Signal-to-Noise Predictions Using VOACAP—A User's Guide*. Cedar Rapids, IA: Rockwell-Collins, 2001.

[26] K. Rawer, *The Ionosphere: Its Significance for Geophysics and Radio Communications*. New York: F. Ungar, 1956.

[27] K. W. Tremellen and J. W. Cox. "The influence of wave propagation on the planning of short-wave communication," *J. Inst. Electr. Eng.*, vol. 94, no. 11, pp. 200–219, Mar.–Apr. 1947.

[28] IPS Radio and Space Services. (2009). *ASAPS for Windows V5.3 tutorial*. [Online]. Available: http://www.sws.bom.gov.au/Category/Products%20and%20Services/Software/ASAPS/ASAPSVer5.3.pdf

[29] International Telecommunication Union. (2014). ITURHFPROP: A software method for the prediction of the performance of HF circuits based on Recommendation ITU-R P.533-12. [Online]. Available: https://www.itu.int/oth/R0A0400006F/en

[30] International Telecommunication Union, "Method for the prediction of the performance of HF circuits," Geneva, Switzerland, Recommendation ITU-R P.533-13, July 2015.

[31] J. L. Lloyd, G. W. Haydon, D. L. Lucas, and L. R. Teters. "Estimating the performance of telecommunication systems using the ionospheric transmission channel. Volume I: Techniques for analyzing ionospheric effects upon HF systems (draft)," U.S. Army Communications Engineering and Installation Agency, Fort Huachuca, AZ, Tech. Rep. EMEOPED-79-7, 1978.

[32] B. A. Witvliet, E. van Maanen, G. J. Petersen, A. J. Westenberg, M. J. Bentum, C. H. Slump, and R. Schiphorst, "Measuring the isolation of the circularly polarized characteristic waves in NVIS propagation," *IEEE Antennas Propag. Mag.*, vol. 57, no. 3, pp. 120–145, June 2015.

[33] J. M. Goodman, *Space Weather & Telecommunications*. New York: Springer, 2005.

[34] National Oceanic and Atmospheric Administration. (2015). [Online]. Available: http://www.ngdc.noaa.gov/stp/IONO/rt-iono/realtime/RL052_foF.png

[35] E. O. Olatunji, "Ionospheric absorption of the extraordinary wave," *Radio Sci.*, vol. 17, no. 5, pp. 1335–1342, Sept./Oct. 1982.

[36] P. A. Bradley, "Limiting polarisation of radio waves of medium and high frequency reflected from the ionosphere," *Proc. Inst. Electr. Eng.*, vol. 114, no. 12, pp. 1837–1841, Dec. 1967.

[37] K. Davies, *Ionospheric Radio Waves*. Waltham, MA: Blaisdell, 1969.

[38] J. D. Kraus, and R. J. Marhefka, *Antennas for All Applications*, 3rd Ed. New York: McGraw-Hill, 2002.

[39] K. G. Budden, *The Propagation of Radio Waves*. Cambridge, U.K.: Cambridge Univ. Press, 1985.

[40] B. A. Witvliet, "Near vertical incidence skywave: Interaction of antenna and propagation mechanism," Ph.D. dissertation, Univ. of Twente, Enschede, The Netherlands, 2015.

[41] G. K. Lott, W. R. Vincent, and S. Jauregui, "HF signal amplitude distributions and total spectrum power measurements," in *Proc. 6th Int. Conf. High Frequency Radio Systems and Techniques*, York, U.K., 1994, pp. 140–143.

[42] International Telecommunication Union, "Radio noise," Geneva, Switzerland, Recommendation ITU-R P.372-12, July 2015.

[43] G. H. Hagn and K. A. Posey, "Survey of literature pertaining to the equatorial ionosphere and tropical communication," Stanford Res. Inst., Menlo Park, CA, Special Tech. Rep. 12, Feb. 1966.

[44] G. H. Hagn, "Orientation of linearly polarized HF antennas for short-path communication via the ionosphere near the geomagnetic equator," Stanford Res. Inst., Menlo Park, CA, Research Memorandum 5 (revised), June 1964.

[45] P. Nacaskul, "Orientation measurements in Thailand with HF dipole antennas for tactical communication," Stanford Res. Inst., Menlo Park, CA, Special Tech. Rep. 31, June 1967.

[46] E. E. Johnson, S. Cook, R. I. Desourdis, G. Earle, and J. C. Ostergaard, *Advanced HF Radio Communications*. Norwood, MA: Artech House, 1997.

[47] E. E. Johnson, E. Koski, W. N. Furman, M. Jorgenson, and J. Nieto, *Third-Generation and Wideband HF Radio Communications*. Norwood, MA: Artech House, 2013.

[48] G. Lane, "Improved guidelines for automatic link establishment operations," in *Proc. Ionospheric Effects Symp. 2005*, Alexandria, VA, 2005, pp. 280–289.

[49] M. C. Walden, "Analysis of Chilton ionosonde critical frequency measurements during solar cycle 23 in the context of midlatitude HF NVIS frequency predictions," in *Proc. 12th Inst. of Engineering and Technology Int. Conf. Ionospheric Radio Systems and Techniques*, York, U.K., 2012.

[50] International Telecommunication Union, "Definitions of maximum and minimum transmission frequencies," Geneva, Switzerland, Recommendation ITU-R P.373-9, Sept. 2013.

[51] L. Barclay, "Outstanding problems for the probabilistic prediction of the performance of HF terrestrial services," in *Proc. 12th Inst. of Engineering and Technology Int. Conf. Ionospheric Radio Systems and Techniques*, York, U.K., 2012.

[52] J. A. Secan and P. J. Wilkinson, "Statistical studies of an effective sunspot number," *Radio Sci.*, vol. 32, no. 4, pp. 1717–1724, July/Aug. 1997.

[53] L. F. McNamara, "Quality figures and error bars for autoscaled digisonde vertical incidence ionograms," *Radio Sci.*, vol. 41, no. 4, p. RS4011, July 2006.

[54] M. C. Walden. Analysis of Chilton ionosonde critical frequency measurements during solar cycle 23 in the context of midlatitude HF NVIS frequency predictions (use of T-Index with VOACAP), in *Proc. High Frequency Industry Assoc. Meeting*, York, U.K., 2012. [Online]. Available: http://www.hfindustry.com/meetings_presentations/presentation_materials/2012_sept_hfia/presentations/10_Plextek_%20hfia2012_york_presentation_mcw_20120906.pdf

[55] R. A. Bamford, R. Stamper, and L. R. Cander, "A comparison between the hourly autoscaled and manually scaled characteristics from the Chilton ionosonde from 1996 to 2004," *Radio Sci.*, vol. 43, no. 1, p. RS1001, 2008.

[56] P. Bhaneja, G. D. Earle, R. L. Bishop, T. W. Bullett, J. Mabie, and R. Redmon, "A statistical study of midlatitude spread F at Wallops Island, Virginia," *J. Geophys. Res.*, vol. 114, no. A4, p. A04301, Apr. 2009.

[57] E. E. Johnson, "NVIS communications during the solar minimum," in *Proc. IEEE Military Communications Conf. 2007*, Orlando, FL, 2007.

[58] L. F. McNamara, R. J. Barton, and T. W. Bullett, "Analysis of HF signal power observations on two North American circuits," *Radio Sci.*, vol. 41, no. 5, p. RS5S38, Apr. 2006.

[59] M. C. Walden, "Comparison of propagation predictions and measurements for mid-latitude HF NVIS links at 5 MHz," in *Proc. 13th Int. Ionospheric Effects Symp.*, Alexandria, VA, 2011, pp. 304–311.

[60] M. C. Walden, "Comparison of propagation predictions and measurements for midlatitude HF near-vertical incidence sky wave links at 5 MHz," *Radio Sci.*, vol. 47, no. 4, p. RS0L09, Aug. 2012.

[61] L. F. McNamara, T. W. Bullett, E. Mishin, and Y. M. Yampolski, "Nighttime above-the-MUF HF propagation on a midlatitude circuit," *Radio Sci*., vol. 43, no. 2, p. RS2004, Mar. 2008.

[62] International Telecommunication Union, "Propagation at frequencies above the basic MUF," Geneva, Switzerland, Recommendation ITU-R P.2011-1, 1999.

[63] International Telecommunication Union, "Method for the prediction of the performance of HF circuits," Geneva, Switzerland, Recommendation ITU-R P.533-12, Sept. 2013.

[64] R. Hanbaba, "Performance prediction methods of HF radio systems," *Ann. Geofis.*, vol. 41, nos. 5–6, pp. 715–742, Nov.–Dec. 1998.

[65] G. Lane. (2016). Understanding above-the-MUF predictions. *VOACAP Quick Guide.* [Online]. Available: http://www.voacap.com/above-muf.html

[66] M. C. Walden. VOACAP reliability (REL) predictions: A sanity check for HF NVIS links, in *Proc. High Frequency Industry Assoc. Meeting*, Portsmouth, U.K., 2014. [Online]. Available: http://www.hfindustry.com/meetings_presentations/presentation_materials/2014_sept_hfia/presentations/1-VOCAP-Reliability.pdf